

# Reliability of the Quark Model in Describing the Strong Light Meson Decays

M. Allosh<sup>1\*</sup>, A. M. Yasser<sup>1</sup>, Atef Ismail<sup>2</sup>

<sup>1</sup>Physics Department, South Valley University, 83523 Qena, Egypt.

<sup>2</sup>Department of Physics, Al-Azhar University, 71524 Assiut, Egypt.

Received: 20 Oct .2020, Revised: 18 Nov .2020, Accepted: 14 Dec. 2020.

Published online: 1 Jan. 20201.

**Abstract:** Study the potential decays of the light–quarks at various incident energies is a method to investigate the meson structure and decay width. The formalism of the quark model is extended to be valid for an arbitrary form of the creation vertex in the presence of the exact meson wave functions. Based on the non–relativistic quark model, the light quark problem is solved. The model is then applied for stable mesons in the final state to be known experimentally. The calculated square roots of the decay width based on two different types of potentials (AL2 and AP2) are in good agreement with the experimental data.

**Keywords:** Light meson, non–Relativistic quark model, Quark model, Decay width.

## 1 Introduction

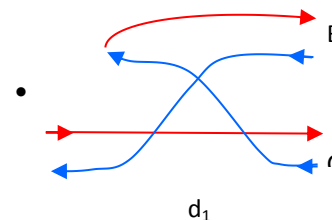
The quark model [1] compares very well with the light quark meson spectrum and meson decays. Certainly, there are disagreements, but many of these deviations attributed to the natural limitations of the model when compared to the inherent complexity of quantum chromodynamics (QCD). However, there are some other prefunded degrees of disagreements which are presumably point out the uncounted features of QCD in the quark model, and may indeed point to the fundamental degrees of freedom needed to fully describe hadron structure. This way may lead to identify the necessary features which will one day have to be met by any purported solution of the full theory.

Light Mesons are built of light flavors (i.e., u, d and s). The constituent masses of these quarks are so similar till the limit that they cannot be distinguished based on their quark content but must be expected to encounter mixed states of all three light flavors. The masses and quantum numbers of the various mesons may also be used to make sense of how these particles decay. Due to the difficulty of using perturbative and non–perturbative QCD in computing the hadronic properties, the properties of hadrons are calculated based on the models inspired by QCD rather than the full theory. Many authors [2–12] successfully applied the quark–pair creation (QPC) model to describe the strong decays of mesons. A good introduction to the model can be found in Refs. [13–15]. In this paper,

Phenomenological in describing ordinary hadrons, more specifically quark–antiquark bound states (mesons).

## 2 The Quark Model

One of the fruitful applications of the quark model into strong decays of hadrons is the well–known QPC model. In this model, meson decay occurs when a quark–antiquark pair is produced from the vacuum in a state suitable for quark rearrangement to occur, as shown in Figure (1). The created pair will have the quantum numbers of vacuum,  $J^{PC} = 0^{++}$ , where  $P$  is the parity and  $C$  is the conjugation of charge [16]. There is one undetermined parameter  $\gamma$  in the model which represents the probability that a quark–antiquark pair will be created from the vacuum. The rest of the model is just the description of the overlap of the initial meson (A) and the created pair (sometimes referred to 0) with the two final mesons (B, C), and to calculate the probability that rearrangement (and hence decay) will occur [17].



\*Corresponding author e-mail: mohe1112013@gmail.com

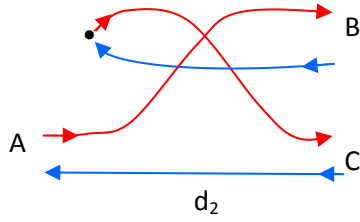


**Fig.1:** Two possible diagrams contributing to the meson decay ( $A \rightarrow BC$ ) in the QPC model.

The study of hadron decays using this model is concerned almost exclusively with numerical predictions, and yet leads to any fundamental modifications. Recent studies considered the changes in the spatial dependence of pair production amplitude as a function of quark coordinates [2, 18, 19] but the fundamental decay mechanism is usually not addressed. In paper [20], a general formulation for any decay is investigated. Here, we skip a lot of technical details in order to focus more on new aspects that are developed.

### 2.1 Meson Wave Function

In a quark model of meson, the wave function describing the relative motion of the quark and antiquark is obtained by solving the Schrödinger equation with a Hamiltonian inspired by QCD [21]. In the non-relativistic approximation, the meson wave function is the eigenfunction of the Schrödinger equation

$$\hat{H}\psi = E\psi, \quad (1)$$

where the Hamiltonian of the system is

$$\hat{H} = K + V_{q\bar{q}}(\vec{r}), \quad (2)$$

where  $K$  is the kinetic energy and  $V_{q\bar{q}}(\vec{r})$  is the effective potential which contains the effects of a Lorentz-vector one-gluon-exchange interaction at short distances and a Lorentz scalar linear confining interaction of the model. To find the meson wave function, Eq. (2) has to be solved as accurately as possible. It is quite easy to solve the differential equation resulting from the Schrödinger equation. However, the radial part  $R_{nls}(\vec{r})$  of the meson wave function is calculated numerically on a grid. This form is not easily used to study more complicated problems. To solve this problem, the regularized part of the exact radial wave function must be approximated by a linear combination of Gaussian functions

$$R_{nls}(\vec{r}) \sum_{i=1}^N c_i \exp(-\alpha_i r^2), \quad (3)$$

This expression is used in the model for meson decays. For a given number  $N$  of Gaussian functions, the parameters  $c_i$  and  $\alpha_i$  are determined by variational procedure on the

energy state;  $N=1$ , which is a rather rough approximation, but for  $N=2$  and  $3$  are massively improve the results [20].

### 2.2 Phase Space

The phase space is the most important factor to calculate the decay width. The most interest part is the partial width  $\Gamma_{A \rightarrow BC}$  corresponding to the decay of meson  $A$  into two mesons  $B$  and  $C$ . A coupling can be adopted based on the angular momentum  $J_{BC}$ , total spin of  $(BC)$  and relative angular momentum  $l$  between  $B$  and  $C$ ,

$$\Gamma_{A \rightarrow BC} = \sum_{J_{BC}, l} \Gamma_{A \rightarrow BC}(J_{BC}, l), \quad (4)$$

where the partial width corresponding to quantum numbers  $J_{BC}$ ,  $l$  is related to the transition amplitude  $M$  through the golden rule,

$$\Gamma_{A \rightarrow BC}(J_{BC}, l) = 2\pi \int dP_0 \delta(E_i - E_f) |M_{A \rightarrow BC}(P_0)|^2, \quad (5)$$

Where  $E_i$  and  $E_f$  are the initial and final energy states for mesons ( $A$ ) and ( $B$  and  $C$ ), respectively. The total width  $\Gamma$  is the sum of partial widths  $\Gamma_{A \rightarrow BC}$  on a given meson-meson channel. This quantity is the sum of partial widths with a given relative angular momentum  $l$  and intrinsic spin of the final state  $J_{BC}$ .

The result for this integral on  $P$ , the relative momentum of  $B$  and  $C$  mesons, depends on which phase space is retained. In this paper, it follows the prescription of [18] and the formula for decay width in the relativistic expression is written as

$$\Gamma_{A \rightarrow BC}(J_{BC}, l) = 2\pi \frac{E_B(P_{rel}) E_C(P_{rel})}{m_A P_{rel}} |M_{A \rightarrow BC}(P_{rel})|^2, \quad (6)$$

$$P_{rel} = \frac{[m_A^2 - (m_B - m_C)^2]^{1/2} [m_A^2 - (m_B + m_C)^2]^{1/2}}{2m_A}, \quad (7)$$

Where  $m$  is the rest of mass,  $E$  is the energy,  $P_{rel}$  is the relative momentum, and

$$E_B(P_{rel}) = \sqrt{m_B^2 + P_{rel}^2},$$

$$E_C(P_{rel}) = \sqrt{m_C^2 + P_{rel}^2},$$

The non-relativistic expression for meson energy  $E = m + (P_{nrel}^2 / 2m)$  and with this prescription, we have

$$\Gamma_{A \rightarrow BC}(J_{BC}, l) = 2\pi \frac{m_B m_C}{(m_B + m_C) P_{nrel}} |M_{A \rightarrow BC}(P_{nrel})|^2, \quad (8)$$

The non-relativistic momentum is given by

$$P_{nrel} = \frac{\sqrt{2m_B m_C (m_A - m_B - m_C)}}{\sqrt{m_B + m_C}}. \quad (9)$$

These expressions are coded into routines in the symbolic computation package Mathematica.

### 3 The Potentials Used

Over the years, several potentials have been used and some of these potentials are found with very crucial test as a unified description of particle spectra. These potentials have been applied on the meson and baryon sectors, and also to tetra-quark states [21, 22]. The resulted data of all cases are encouraging. In this paper, two potentials [23] that yield good overall results for the meson spectrum are used in the study. The use of different potentials allows us to check the sensitivity of our results and the inter-quark interaction. The general form of each potential is more or less imposed by some basic QCD constraints, but the parameters are determined by a fit to a well-chosen sample of light meson states. Both potentials rely on a non-relativistic expression of the kinetic energy operator, and they need to solve the Schrödinger equation using the Numerov algorithm [24–29]. as well as they take the general form

$$V_{q\bar{q}}(r) = -\frac{k(1-\exp(-\frac{r}{r_c}))}{r} + \lambda r^p - \Lambda + \left( \frac{2\pi k}{3m_q m_{\bar{q}}} \left( 1 - \exp\left(-\frac{r}{r_c}\right) \frac{\exp\left(-\frac{r^2}{r_0^2}\right)}{\pi^{3/2} r_0^3} \right) \vec{\sigma}_q \vec{\sigma}_{\bar{q}} \right), \tag{10}$$

Where  $\vec{\sigma}_q, \vec{\sigma}_{\bar{q}}$ , are the Pauli matrices. One characteristic of these potentials is that the range  $r_0$  of the hyperfine term is mass dependence through the relation.

$$r_0(m_q m_{\bar{q}}) = a \left( \frac{2m_q m_{\bar{q}}}{m_q + m_{\bar{q}}} \right)^{-b}, \tag{11}$$

The letter A means "for All mesons". The letter L or P denotes as the Linear or the 2/3-Power confinement, respectively; the number 2 indicates that the parameter  $r_c$  is not equal to zero [23].

### 4 Results and Discussion

The theoretical square roots of the decay width for some light mesons are calculated based on two types of potentials as explained on the above context. The obtained results are compared to new published experimental data [30]. These new results are fitted by using the experimental spectra to give the most suitable decay widths with experiments. The  $\chi^2$  relation is used to easily compare among the results obtained by using potentials AL2 and AP2, and this relation is defined as

$$\chi^2 = \frac{1}{n} \sum_{k=1}^n (\Gamma_k^{1/2, theo.} - \Gamma_k^{1/2, Exp.})^2, \tag{12}$$

In this formula, the summation runs over a selected sample of  $n$  mesons in the group. The value  $\Gamma_k^{1/2, Exp.}$  is the experimental square root of the decay width for meson labeled  $k$  in the sample, while  $\Gamma_k^{1/2, theo.}$  is the corresponding theoretical square root of the decay width depending on the free parameters. The formalism must be developed to study the influence of the creation vertex  $\gamma(p)$  for the description

of the transition. This study is carried out using two different forms depending on several parameters

$$\gamma(p) = A, \tag{13}$$

Most authors have used a constant expression in Eq. (13) [20] essentially for simplicity and because of the results are corrected therefore the expression

$$\gamma(p) = AB e^{-Cp^2}. \tag{14}$$

In fact, one aim of this paper is to explore the gain obtained in the framework of Eq. (14) compared to the traditional Eq. (13) via two different potential wave functions. Only one parameter  $A$  appears in Eq. (13), while, there are three parameters  $A, B$  and  $C$  in case of Gaussian vertex as shown in Eq. (14). The parameters of  $nn^{\bar{}}$  vertex (in the following  $n$  denotes generically a member of the isospin doublet  $u$  or  $d$ ) are obtained by fitting the first seven transitions in Table I, while the parameters of  $ss^{\bar{}}$  vertex are obtained by fitting the next three transitions in Table 1. Since predominating the transitions related to either  $nn^{\bar{}}$  or  $ss^{\bar{}}$  creations, and the fit is conducted over the square of the amplitude, the sign of the vertex is irrelevant. Several criteria are used the expression (14) and some selected transitions are listed in Table 1.

Table 1: Transitions used to determine the parameters of  $\gamma(p)$

Transition
$f_2(1270) \rightarrow \pi \pi$
$\bar{f}_2(1525) \rightarrow k \bar{k}$
$\phi \rightarrow k \bar{k}$
$k_2^*(1425) \rightarrow k \pi$
$k_2^*(1425) \rightarrow k \rho$
$k_2^*(1425) \rightarrow k^*(892) \pi$
$k^*(892) \rightarrow k \pi$
$a_2 \rightarrow k k$
$f_2(1270) \rightarrow k \bar{k}$
$f_4(2050) \rightarrow k \bar{k}$

In case of a Gaussian vertex Eq. (14), to determine the parameters  $A_s, B_s$  and  $C_s$  describing  $ss^{\bar{}}$  creation, we have to fit on 3 transitions. In order to determine the parameters  $A_n, B_n$  and  $C_n$  describing  $nn^{\bar{}}$  creation, we conducted the fit on five transitions. In practice, in order to keep some consistencies for the whole set of results, the form  $k_2^*(1425) \rightarrow k \rho$  and  $k_2^*(1425) \rightarrow k^*(892)\pi$ , is removed from the set of seven transitions being considered because they contain a broad meson in the final state. In general, we call a broad meson as a meson with width larger than 50 MeV.

For the sake of calculations, the experimental masses of mesons are considered. To avoid giving too much importance to the well measured transitions, the weight used in  $\chi^2$  is considered. To avoid too large dispersion of the results, the square roots of the width corresponding to the given transitions are measured. It is more convenient to produce  $\chi^2$  based on  $\Gamma^{1/2}$  to conform more closely to the

experimental platform. It also gives the absolute chi-square ( $\chi^2$ ) and the chi-square per degree of freedom ( $\chi^2/\text{d.o.f.}$ ). In Tables 2 and 3, the results are gathered based on AL2 and AP2 potentials by using relativistic and non-relativistic phase space for both constant and Gaussian vertices when mesons appear in the final state with small width. Figures 2 and 3, illustrate a comparison between experimental data and calculations based on the relativistic phase space. Same comparison is shown in Figures 4 and 5 for the non-relativistic phase space.

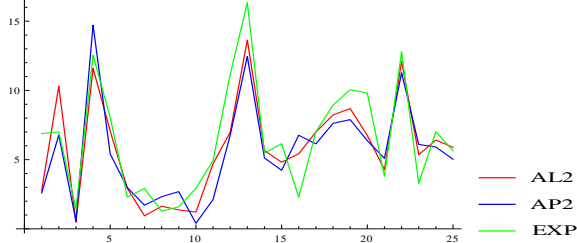


**Fig.2:** Theoretical square root of decay width for constant function versus the experimental data using relativistic phase space.

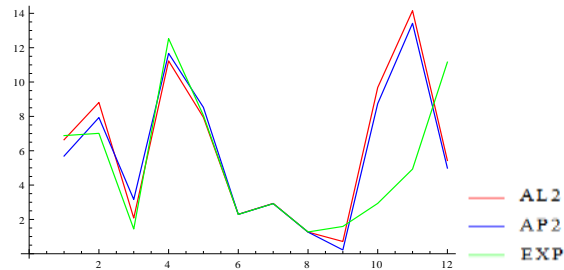


**Fig.3:** Theoretical square root of decay width for Gaussian vertex function versus the experimental data using relativistic phase space.

Differences between AL2 and AP2 potentials are more pronounced. AL2 is slightly better on average when using relativistic phase space and using Gaussian vertex function, while for non-relativistic phase space and Gaussian vertex function, AP2 is better on average. Finally, one can allege that the results with relativistic phase space are better than the results using non-relativistic phase space, and this is acceptable for the small particles.

**Table 2:** Calculated square root of decay width of stable mesons in the final state for constant and Gaussian vertex functions. The AL2, AP2 potentials and relativistic phase space are used. The last column contains the experimental square root of the width.

Decay	$\gamma = A$		$\Gamma^{1/2}$ [MeV]		Exp.
	AL2	AP2	$\gamma = A + B e^{-cp^2}$		
	AL2	AP2	AL2	AP2	
$k^*(892) \rightarrow k \pi$	2.77	2.59	6.64	5.69	6.88
$k_2^*(1425) \rightarrow k \pi$	10.03	6.77	8.81	7.93	7.01
$\varphi(1020) \rightarrow k \bar{k}$	0.47	0.59	2.08	3.16	1.44
$f_2(1270) \rightarrow \pi \pi$	11.59	14.71	11.23	11.67	12.53
$\bar{f}_2(1525) \rightarrow k \bar{k}$	7.07	5.41	7.94	8.52	8.05
$a_2(1320) \rightarrow k k$	2.92	2.98	2.30	2.29	2.29
$f_2(1270) \rightarrow k \bar{k}$	0.94	1.71	2.93	2.92	2.92
$f_4(2050) \rightarrow k \bar{k}$	1.63	2.32	1.26	1.26	1.27
$\rho_3(1690) \rightarrow k k$	1.37	2.69	0.713	0.22	1.59
$k_2^*(1425) \rightarrow k \rho$	1.21	0.40	-	-	2.93
$k_2^*(1425) \rightarrow k^* \pi$	4.70	2.11	-	-	4.93
$k^*(1680) \rightarrow k \pi$	6.98	6.76	9.68	8.74	11.16
$k_0^*(1430) \rightarrow k \pi$	13.64	12.45	14.16	13.42	16.34
$k_3^*(1780) \rightarrow k \pi$	5.66	5.12	5.43	4.99	5.47
$k_1(1270) \rightarrow k \rho$	4.81	4.23	-	-	6.15
$k_1(1400) \rightarrow k \rho$	5.43	6.76	-	-	2.28
$\pi_2(1670) \rightarrow \rho \pi$	6.99	6.14	-	-	7.02
$\pi_2(1670) \rightarrow \rho \pi$	8.23	7.62	-	-	8.94
$k^*(1680) \rightarrow k \rho$	8.69	7.89	-	-	10.06
$k^*(1680) \rightarrow k^* \pi$	6.75	6.37	-	-	9.81
$k_1(1270) \rightarrow k^* \pi$	4.28	5.09	-	-	3.80
$k_1(1400) \rightarrow k^* \pi$	12.11	11.27	-	-	12.79
$\pi_2(1670) \rightarrow k k^*$	5.36	6.10	-	-	3.29
$k_3^*(1780) \rightarrow k \rho$	6.41	5.91	-	-	7.02
$k_3^*(1780) \rightarrow k^* \pi$	5.89	5.02	-	-	5.64
$\chi^2$	33.12	45.22	5.41	6.19	
$\chi^2/\text{d.o.f.}$	5.52	7.54	1.35	1.55	

**Table 3:** Theoretical square root of the decay width of stable mesons in the final state for constant and Gaussian vertex functions; The AL2, AP2 potentials and non-relativistic phase space are used. The last column contains the experimental square root of the decay width.

Decay	$\Gamma^{1/2}$ [MeV]				Exp.
	$\gamma = A$		$\gamma = A + B e^{-cp^2}$		
	AL2	AP2	AL2	AP2	
$k^*(892) \rightarrow k \pi$	4.31	5.35	3.13	6.58	6.88
$k_2^*(1425) \rightarrow k \pi$	6.44	5.77	6.00	7.95	7.01
$\varphi(1020) \rightarrow k \bar{k}$	1.29	2.21	1.62	3.07	1.44
$f_2(1270) \rightarrow \pi \pi$	4.71	7.88	7.02	13.73	12.53
$\bar{f}_2(1525) \rightarrow k \bar{k}$	12.50	12.67	5.95	10.65	8.05
$a_2(1320) \rightarrow k k$	2.93	3.23	3.35	1.52	2.29
$f_2(1270) \rightarrow k \bar{k}$	0.98	2.29	1.19	1.92	2.92
$f_4(2050) \rightarrow k \bar{k}$	2.94	4.35	3.04	0.21	1.27
$\rho_3(1690) \rightarrow k k$	1.88	4.24	1.65	2.79	1.59
$k_2^*(1425) \rightarrow k \rho$	2.07	1.29	-	-	2.93
$k_2^*(1425) \rightarrow k^* \pi$	4.39	2.43	-	-	4.93
$k^*(1680) \rightarrow k \pi$	3.89	8.21	9.30	10.41	11.16
$k_0^*(1430) \rightarrow k \pi$	8.04	3.23	8.65	12.95	16.34
$k_3^*(1780) \rightarrow k \pi$	5.24	2.17	4.13	4.78	5.47
$k_1(1270) \rightarrow k \rho$	2.22	4.47	-	-	6.15
$k_1(1400) \rightarrow k \rho$	4.51	3.58	-	-	2.28
$k_3^*(1780) \rightarrow k \rho$	8.12	3.28	-	-	7.02
$\pi_2(1670) \rightarrow \rho \pi$	5.32	2.85	-	-	8.94
$k^*(1680) \rightarrow k \rho$	10.3	4.15	-	-	10.06
$k^*(1680) \rightarrow k^* \pi$	2.32	8.71	-	-	9.81
$k_1(1270) \rightarrow k^* \pi$	1.65	6.61	-	-	3.80
$k_1(1400) \rightarrow k^* \pi$	5.23	6.81	-	-	12.79
$\pi_2(1670) \rightarrow k k^*$	5.99	2.94	-	-	3.29
$k_3^*(1780) \rightarrow k \rho$	4.26	6.30	-	-	7.02
$k_3^*(1780) \rightarrow k^* \pi$	6.57	3.70	-	-	5.64
$\chi^2$	88.87	56.36	10.08	2.88	
$\chi^2/d.o.f.$	14.81	9.39	2.52	0.72	

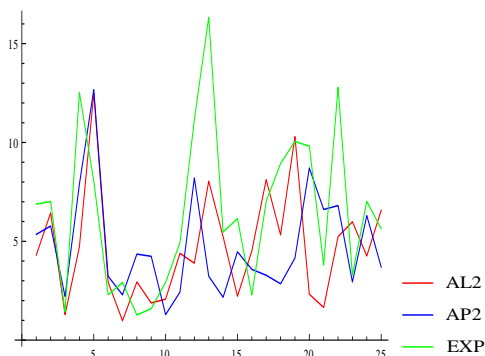


**Fig.4:** Theoretical square root of decay width for constant function versus the experimental data using non-relativistic phase space.

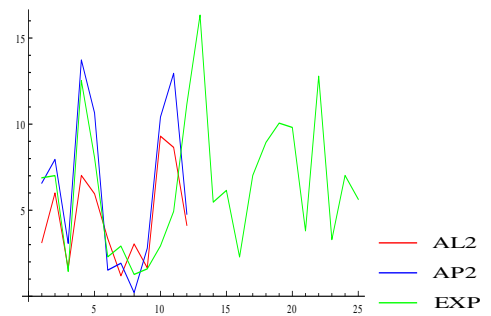


**Fig.5:** Theoretical square root of decay width for Gaussian vertex function versus the experimental data using non-relativistic phase space.

## 5 Conclusions

Predictive power of theory requires good models and accurate calculation methods. It is desirable for theorist to make predictive suggestion to experiments in quicker developing fields. In this work, the most sophisticated calculations in the framework of QPC model are presented. The meson wave functions are calculated by using the non-relativistic potential. Although it is computed by using Numerov's algorithm, which is very precise, we have done a fit to express them as a sum of Gaussian functions. In this paper, both potentials (AL2 and AP2) are considered. In general, a good agreement between the predicted and experimental data is found. Both potentials reproduce decay width with comparable quality. Finally, it worth concluding that the most important ingredient of the QPC mechanism relies on suitable description of the vertex. However, the QPC model with a dynamical vertex  $\gamma(p)$  is very suitable for the study of strong transitions.

## References

- [1] W. Roberts and B. Silvestre-Brac, General method of calculation of any hadronic decay in the 3 P 0 model, *Few-Body Systems.*, **11**, 171 (1992).
- [2] P. R. Page, Excited charmonium decays by flux-tube breaking and the  $\psi'$  anomaly at CDF, *Nucl. Phys.*, **B 446**, 189 (1995).
- [3] S. Capstick and N. Isgur, Baryons in a relativized quark model with chromodynamics, *Phys. Rev.*, **D 34**, 2809 (1986).
- [4] S. Capstick and W. Roberts, Quasi-two-body decays of non-strange baryons, *Phys. Rev.*, **D 49**, 4570 (1994).
- [5] E. S. Ackleh, T. Barnes and E. S. Swanson, On the mechanism of open-flavor strong decays, *Phys. Rev.*, **D 54**, 6811 (1996).
- [6] H. Q. Zhou, R. G. Ping and B. S. Zou, Mechanisms for  $\chi_{cJ} \rightarrow \phi \phi$  Decays, *Phys. Lett.*, **B 611**, 123 (2005).
- [7] X. H. Guo, H. W. Ke, X.Q. Li, X. Liu and S. M. Zhao, *Commun. Theo. Phys.*, **48**, 509 (2007)
- [8] F. E. Close and E. S. Swanson, Dynamics and decay of heavy-light hadrons, *Phys. Rev.*, **D 72**, 094004 (2005)
- [9] J. Lu, W.Z. Deng, X. L. Chen and S.L. Zhu, Pionic decays of  $D_{sJ}$  (2317),  $D_{sJ}$  (2460) and  $B_{sJ}$  (5718), *Phys. Rev.*, **D 73**, 054012 (2006)
- [10] B. Zhang, X. Liu, W.Z. Deng and S.L. Zhu,  $D_{sJ}$  (2860) and  $D_{sJ}$  (2715), *Eur. Phys. J. C* **50**, 617 (2007)
- [11] X. Liu, C. Chen, W.Z. Deng and X.L. Chen, NASA Tech Briefs, *Chin. Phys. C (HEP& NP)* ., **32(10)**, Oct. (2008)
- [12] A. Le Yaouanc, L. Oliver, O. Pene and J. Raynal, Naïve Quark-Pair-Creation Model of Strong-Interaction Vertices, *Phys. Rev.*, **D8**, 2223 (1973).
- [13] A. Le Yaouanc, L. Oliver, O. Pene and J. Raynal, Naive quark pair creation model and baryon decays, *Phys. Rev.*, **D9**, 1415 (1974).
- [14] A. Le Yaouanc, L. Oliver, O. Pene and J. Raynal, Strong decays of  $\psi$ dblac; (4.028) as a radial excitation of charmonium, *Phys. Rev.*, **D11**, 1272 (1977).
- [15] L. Micu, Decay rates of meson resonances in a quark model, *Nucl. Phys.*, **B10**, 521 (1969).
- [16] B. Gell-Mann, A schematic model of baryons and mesons, *Phys. Lett.*, **8**, 214 (1964).
- [17] P. Geiger and E. S. Swanson, Distinguishing among strong decay models, *Phys. Rev.*, **D50**, 6855 (1994).
- [18] W. Roberts, B. Silvestre-Brac, Meson decays in a quark model, *Phys. Rev.*, **D57**, 1964 (1998).
- [19] Stephen Godfrey and Nathan Isgur, Mesons in a relativized quark model with chromodynamics *Phys. Rev.*, **D 32**, 189 (1985).
- [20] R. Bonnaz and B. Silvestre -Brac, Discussion of the 3P0 Model Applied to the Decay of Mesons into Two Mesons, *Few Body Systems.*, **27**, 163 (1999).
- [21] H. G. Blundell, S. Godfrey and Brian Phelps, *Phys. Rev.*, **D 53**, 3712 (1996).
- [22] A. M. Yasser, M. A. Allosh, M. K. Abu-Assy and Ch. C. Moustakidis, Determining Masses of Light Mesons by Using Numerov's Discretization, *Quant. Phys. Lett.*, **6(1)**, 37 (2017).
- [23] R. K. Bhaduri, L.E. Cohler, Y. Nogami, Quark Confinement and the Hadron Spectrum, *Nuovo Cimento.*, **A 65**, 376 (1981) .
- [24] J. M. Blatt, "Practical points concerning the solution of the Schrödinger equation", *J. Comput. Phys.*, **1**, 382-396 (1967).
- [25] A. C. Allison, "The Numerical solution of coupled differential equations arising from the Schrödinger equation", *J. Comput. Phys.*, **6**, 378 (1970).
- [26] D. R. Hartree, The calculations of atomic structures, Wiley, New York (1957).
- [27] A. M. Yasser and G. S. Hassan and T. A. Nahool, Numerical Study of Heavy Meson's Spectra Using the Matrix Numerov's Method, the *International Journal of New Horizons in Physics.*, **2**(2014).
- [28] A. M. Yasser and G. S. Hassan and T. A. Nahool, Theoretical Calculations for Predicted States of Heavy Quarkonium via Non-Relativistic Frame Work, *Electronic Journal of Theoretical Physics.*, **12** (2014).